Paracrine effects of the senescence-associated secretory phenotype decrease cancer cell adhesion

Aidan R. Cole[1], Raquel Buj[1], Amal Taher Elhaw[2,3], Apoorva Uboveja[1], Naveen Tangudu[1], Steffi Oesterreich[1], Wayne Stallaert[4], Nadine Hempel[2], and Katherine M. Aird[1,2*]

[1]Department of Pharmacology & Chemical Biology and UPMC Hillman Cancer Center, University of Pittsburgh School of Medicine, Pittsburgh, PA

[2]Division of Hematology/Oncology, Department of Medicine, and UPMC Hillman Cancer Center, University of Pittsburgh School of Medicine, Pittsburgh, PA

[3]Department of Pharmacology, College of Medicine, Pennsylvania State University, Hershey, PA, USA.

[4]Department of Computational and Systems Biology and UPMC Hillman Cancer Center, University of Pittsburgh School of Medicine, Pittsburgh, PA

*Corresponding Author

Correspondence:
Katherine M. Aird
Associate Professor
UPMC Hillman Cancer Center
Department of Pharmacology & Chemical Biology
University of Pittsburgh School of Medicine
5051 Centre Ave.
Office: 2041; Lab: 2050
Pittsburgh, PA 15213
412-648-4823
katherine.aird@pitt.edu

Keywords: spheroids, adhesion, detachment, dissemination, senescence, secretion

ABSTRACT

High grade serous ovarian cancer (HGSOC) is the most lethal gynecological cancer. Platinum-based therapies such as cisplatin are standard-of-care for HGSOC patients; however, the majority of HGSOCs initially treated with cisplatin will recur with widespread disseminated disease. Cisplatin induces cellular senescence, a stable cell cycle arrest. Although they are non-proliferative, senescent cells secrete a complex mix of cytokines and small molecules, named the senescence associated secretory phenotype (SASP), that have been shown to have pro-tumorigenic effects. To investigate how the SASP contributes to HGSOC progression, we used conditioned media from cisplatin therapy-induced senescent cells to culture naïve HGSOC spheroids. We report that while the SASP does not affect spheroid formation, the adhesion of cells within spheroids is altered, leading to cell detachment from spheroids. Interestingly, our data indicate that this occurs in an MMP-independent manner. Analysis of RNA-Seq samples indicates many adhesion-related genes and adhesion factors are transcriptionally downregulated by the SASP, particularly fibronectin and integrins, which was validated by immunofluorescence in spheroids. These data reveal that senescent cells contribute to a transcriptional program in nearby cancer cells in a paracrine fashion that decreases their adhesion, which may contribute to tumor dissemination.

INTRODUCTION

High grade serous ovarian cancer (HGSOC) is the most lethal gynecological cancer (Torre et al. 2018). ~90% of HGSOC deaths result from disease that recurs after treatment, and these patients all have disseminated disease (Amate et al. 2013). This dissemination occurs most frequently through the transcoelomic route, defined as shedding into the peritoneal cavity (Tan, Agarwal, and Kaye 2006; Lengyel 2010). While the initial dissociation step of this dissemination route is considered passive, it has been associated with the loss of E-cadherin and alpha-catenin, along with changes in other cell-cell adhesion factors (Sawada et al. 2008; Lau, So, and Leung 2013; Myong 2012; Lee et al. 2008; Comamala et al. 2011; Fujimoto et al. 1997). Interestingly, metastasis still occurs through transcoelomic dissemination from peritoneal tumor nodules in recurrence in debulked patients (McPherson et al. 2016) and may be aggravated by chemotherapy (Davidson et al. 2006). Analysis of malignant cells from the peritoneal cavity has identified increased tumorigenesis and cancer stem cell-like characteristics in chemoresistant compared to chemonaïve patients (Latifi et al. 2012). However, little is understood about the role of chemotherapy in promoting metastatic recurrence.

For HGSOC to disseminate, tumor cells must detach and survive in the intraperitoneal space, a non-adherent environment, until they attach to and invade the mesothelium. This coincides with the presence of ascites fluid buildup, which helps carry ovarian cancer cells in multicellular aggregates and spheroids to organs within the peritoneal cavity (Kipps, Tan, and Kaye 2013). The passive dissemination results in peritoneal carcinomatosis (Coccolini et al. 2013). To recapitulate the early stages of HGSOC dissemination, spheroid culture using poly(2-hydroxyethyl methacrylate) [poly-HEMA] ultralow attachment (ULA) plates is often utilized (Yee et al. 2022; Ritch et al. 2022). Flat bottom ULA plates have been used to recapitulate the cell states and

chemoresistance associated with malignant ascites formation (Casagrande et al. 2021). Round bottom ULA plates have been used to model the early adhesion of HGSOC spheroids (Boylan et al. 2020) and as a tool to pre-form spheroids for drug development and to study ovarian cancer cell detachment (Singh et al. 2020; Al Habyan et al. 2018). In this study, we used these *in vitro* systems to assess the adhesion and detachment properties of HGSOC spheroids.

Current standard-of-care therapies for HGSOC are platinum-based therapies (such as cisplatin/carboplatin, which is combined with taxane) or poly (ADP-ribose) polymerase inhibitors (PARPi) (Della Pepa et al. 2015). While these therapies decrease tumor burden, they also induce cellular senescence (Fleury et al. 2019; Paffenholz et al. 2022; Demaria et al. 2017), which can be a double-edged sword in cancer. Cellular senescence is defined as a stable cell cycle arrest, and therefore senescence was initially thought to be a beneficial therapeutic response (Kalathur, Di Mitri, and Alimonti 2015; Perez-Mancera, Young, and Narita 2014; Acosta and Gil 2012). Recent evidence has demonstrated that suppression of senescence inhibits tumorigenesis and chemoresistance (Demaria et al. 2017; Alimirah et al. 2020). This is due in part to the unique secretome of senescent cells, termed the senescence associated secretory phenotype (SASP), that is composed of a variety of pro-inflammatory and pro-tumorigenic factors (Ritschka et al. 2017; Sparmann and Bar-Sagi 2004; Kuilman et al. 2008; Wiley et al. 2016). There is growing evidence that senescence and the SASP in ovarian cancer can promote dissemination (Veenstra, Bittencourt, and Aird 2022). Studies have shown that cytokines IL-6 and IL-8 are both known to enhance ovarian cancer dissemination through JAK/STAT3 signaling and through induction of anoikis resistance (Wen et al. 2014; Mehner et al. 2020; Lane et al. 2011), though these studies were independent of senescence induction. Senescence has been explored in the context of cancer and has been shown to lead to a number of deleterious cancer phenotypes,

specifically metastasis (Acosta and Gil 2012; Coppe et al. 2010; Rodier and Goldstein 2008; Krtolica et al. 2001; Parrinello et al. 2005; Tsai et al. 2005), though often studied in the context of direct remodeling of the extracellular matrix through the increased expression of matrix metalloproteinases (MMPs) in the SASP (Parrinello et al. 2005; Liu and Hornsby 2007; Tsai et al. 2005; Camphausen et al. 2001; Qian et al. 2002). Whether and how the SASP affects ovarian cancer dissemination has not been fully uncovered.

Here we used *in vitro* spheroid models to investigate how the SASP from cisplatin-induced senescent HGSOC cells impacts adhesion and detachment in a paracrine fashion. Analysis of spheroids cultured in senescent conditioned media (SCM) demonstrated an increase in the number of spontaneously formed spheroids without overall changes in viability. This was not due to MMPs as similar results were observed in heat inactivated media, which denatures and inactivates MMPs. Timelapse imaging revealed that SCM induced cellular detachment from the main spheroid body. Finally, HGSOC cells cultured in SCM showed transcriptional downregulation of genes related to cell-cell and cell-ECM adhesion, which was confirmed in spheroids by IF. Together, our data show that the SASP from cisplatin-induced senescent cells contributes to cell-intrinsic changes in adhesion and detachment, which has implications in HGSOC dissemination.

RESULTS

The SASP decreases adhesion in spheroids

We aimed to determine the paracrine effects of therapy-induced senescent cells on naïve HGSOC cells. Towards this goal, we induced senescence in Ovcar8 HGSOC cells using cisplatin, which was confirmed with senescence-associated β-galactosidase activity (SA-β-gal), decreased Lamin B1 expression, increased DNA damage foci (**Fig. 1A-D**). We also confirmed increased senescence-associated secretory phenotype (SASP) cytokine gene expression and secretion (**Fig. 1E-F**). Consistent with the idea that much of the SASP is transcriptionally regulated, Gene Set Enrichment Analysis (GSEA) of cisplatin-treated RNA-Seq samples demonstrated

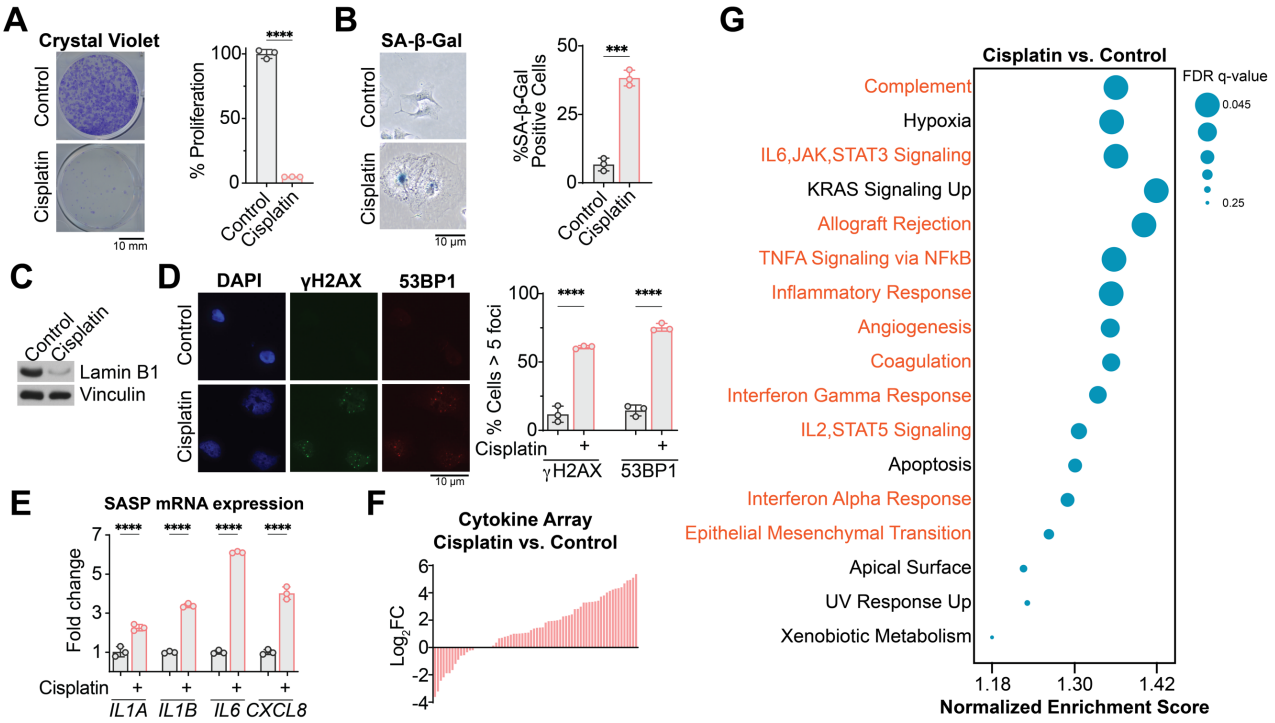

Figure 1. Cisplatin induces senescence and the senescence-associated secretory phenotype (SASP) in Ovcar8 HGSOC cells. Ovcar8 cells treated with 1 µM cisplatin for 48 hours, washed out, and then used to condition media for 48 hours. **A)** Crystal violet proliferation assay and quantification. One of 3 independent experiments is shown. **B)** Senescence-associated-beta-galactosidase (SA-β-Gal) activity and quantification. One of 3 experiments is shown. **C)** Western blot of Lamin B1. Vinculin was used as a loading control. One of three independent experiments is shown. **D)** Immunofluorescence and quantification of 53BP1 and γH2AX foci. One of three independent experiments is shown. **F)** Secretion of cytokines by cytokine array. One independent experiment in technical duplicates. **G)** GSEA analysis enriched pathways of RNA-Seq data. Pathways highlighted in red are related pathways associated with the SASP. T-test, ***p < 0.001, ****p < 0.0001.

many of the top upregulated signatures were related to the SASP, including inflammation, wound healing, angiogenesis, and epithelial to mesenchymal transition (**Fig. 1G and Table S1**). Together, these data show that cisplatin induces senescence in Ovcar8 HGSOC cells and results in robust upregulation and secretion of SASP-associated factors.

Interaction with the ECM and adhesion is important for HGSOC dissemination (Valmiki et al. 2021). Tumor cells detach and survive in the intraperitoneal space, a non-adherent environment, before attaching to and invading the mesothelium (Tan, Agarwal, and Kaye 2006). To investigate the role of the cisplatin-induced SASP in non-adherent conditions, we used ultra-low attachment (ULA) plates, in which HGSOC cells form spontaneous spheroids (Yee et al. 2022; Ritch et al. 2022). We cultured naïve HGSOC cells in spheroids in proliferative conditioned media (PCM) or senescent conditioned media (SCM) (**Fig. 2A**). Culturing HGSOC cells in SCM led to an increased number of spheroids formed when compared to PCM (**Fig. 2C-B**). Spheroids in SCM were also smaller compared to the spheroids formed in PCM, and more single cells or small multicellular aggregates were present (**Fig. 2D**). However, the overall viability of cells in spheroids was unchanged by conditioned media (**Fig. S1**), suggesting the SASP does not promote anoikis resistance in this context. Matrix metalloproteinases (MMPs) are a known part of the SASP (Coppe et al. 2010). Although many of the MMPs are not expressed in Ovcar8s, and we did not observe major differences in MMP gene expression in cisplatin-induced senescence HGSOC cells (**Table S2**), we controlled for potential increased MMP secretion through heat inactivated CM by boiling for 20 minutes at temperatures above MMPs melting points (Meraz-Cruz et al. 2020). Interestingly, we observed similar phenotypes in heat inactivated SCM (**Fig. 2B-D**), suggesting that the SASP confers additional changes in adhesion beyond ECM degradation. To determine if the observed changes in adhesion impact spheroid formation, we used round bottom ULA plates to force non-adherent cells to interact in a small area (**Fig. 2E**). The formation

and compaction of spheroids in round bottom ULA plates were not dependent on the presence of the SASP (**Fig. 2F**). Together, these data show that while formation of spheroids is not affected by the SASP, the adhesion of cells in the spheroid may be altered.

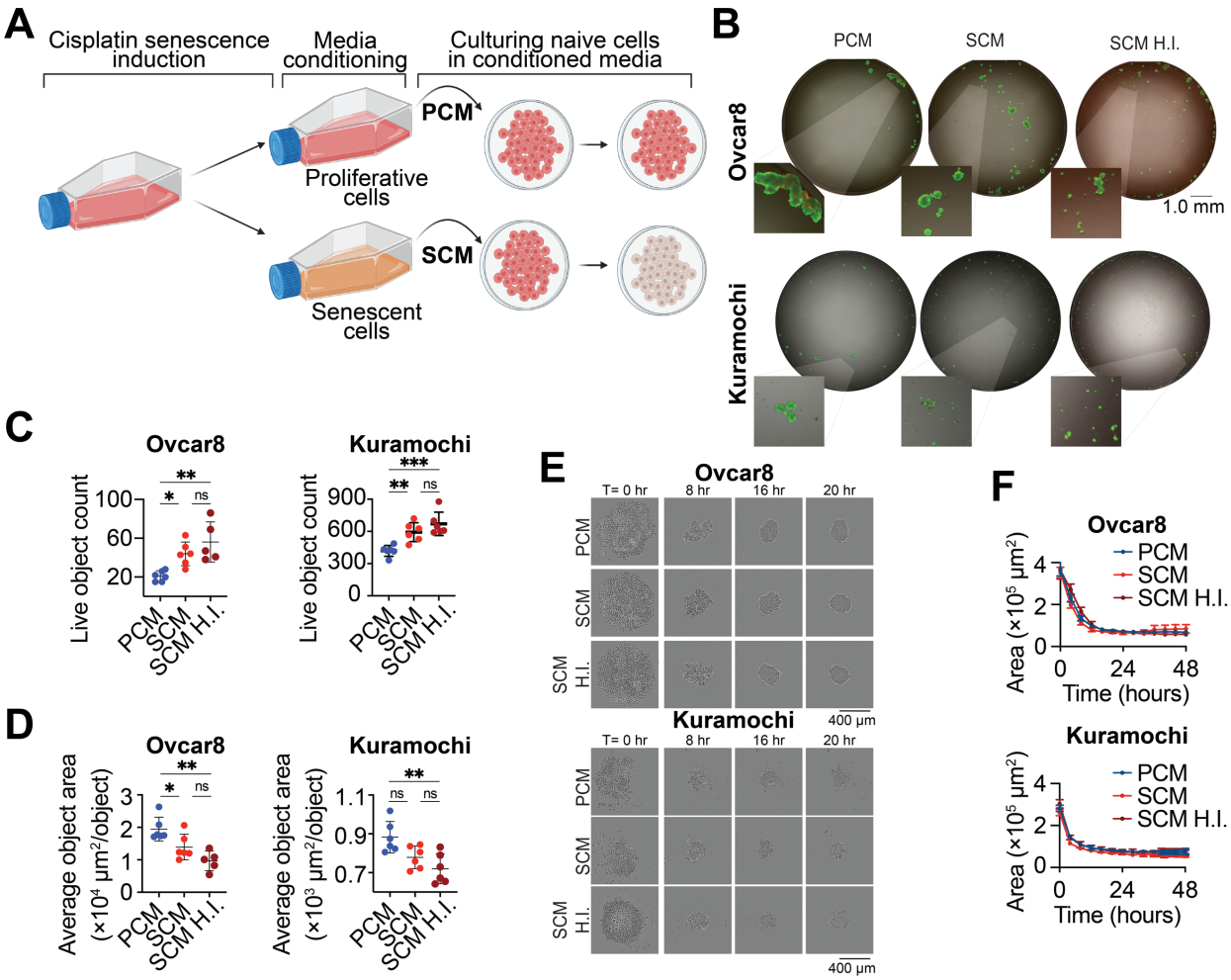

Figure 2. The SASP decreases adhesion of HGSOC spheroids but does not inhibit spheroid formation. A) Schematic of conditioned media formation, collection, and treatment from cisplatin-induced senescent cells (SCM) or control proliferative cells (PCM). **B)** Representative images of spheroids spontaneously formed in flat bottom ULA plates stained with calcein AM (green, live cell stain) and ethidium homodimer (red, dead cell stain) to determine viability. **C-D)** Quantification of live spheroid quantity (**C**) and average size (**D**) per well in **B**. One of 5 independent experiments in Ovcar8 and 3 independent experiments in Kuramochi is shown. **E**) Representative live cell imaging of spheroid formation and compaction in round bottom ULA plates. **F)** Quantification of spheroid area from **E**. One of 3 independent experiments in Ovcar8 and 2 independent experiments in Kuramochi is shown. One-way ANOVA, ns = not significant, *$p < 0.05$, **$p < 0.01$, ***$p < 0.001$.

The SASP increases detachment in spheroids

Since our data indicate that the SASP does not affect spheroid formation (**Fig. 2**), we investigated its role in detachment. Towards this goal, spheroids of equivalent cell number and size were formed in round bottom ULA wells before being transferred to flat bottom ULA wells, after which we performed timelapse imaging (**Fig. 3A**). We observed an increase in the total number of live detachment events when cells were grown in SCM and in heat inactivated SCM (**Fig. 3B-C** and **Video S1**). These data indicate that cell intrinsic changes induced by the SASP weaken adhesion within spheroids and drive cellular detachment.

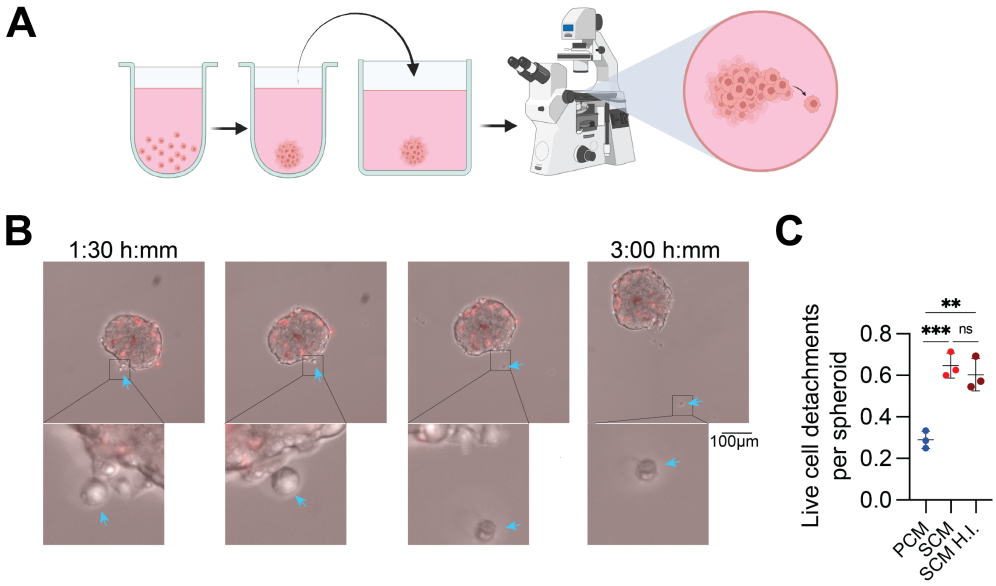

Figure 3. The SASP increases spontaneous cellular detachment from spheroids. A) Schematic of experimental protocol to measure detachment events. **B)** Representative timelapse images of a cell detaching from a spheroid (Ovcar8 cells). **C)** Quantification of detachment events in **B**. One of 2 independent experiments is shown. One-way ANOVA, **p < 0.01, ***p < 0.001.

The SASP decreases ECM and adhesion factors

Our data indicate that the SASP induces cells to detach from spheroids (**Fig. 3**). To gain a more global understanding of the transcriptional signatures associated with these changes, we performed RNA-Seq on HGSOC cells cultured in SCM and PCM and assessed signatures related to ECM and adhesion. Indeed, we uncovered significant negative enrichment of both the KEGG

ECM receptor interaction and KEGG focal adhesion gene sets in cells cultured in SCM compared to PCM (**Fig. 4A and Table S3**). Interestingly, leading edge genes from these signatures were associated with fibronectin, integrins, collagens, and laminins (**Fig. 4B-C**). To further investigate the ECM and adhesion factors in spheroids generated in conditioned media, we performed

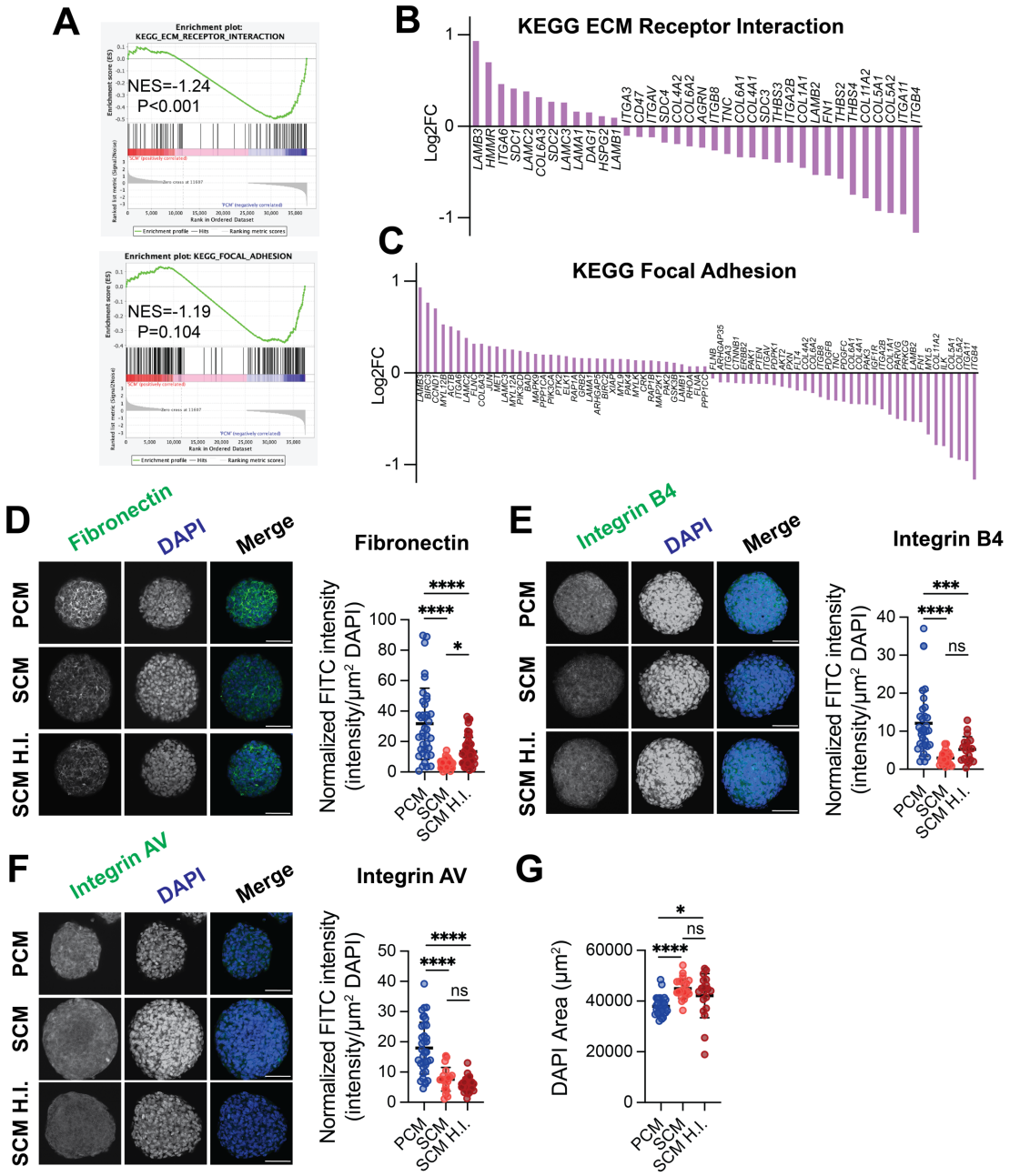

Figure 4. SASP decreases expression of adhesion factors. A) Enrichment plots from GSEA of RNA-Seq data from spheroids cultured in SCM vs. PCM. **B-C)** mRNA expression of genes in the negatively enriched pathways in **A**. **D-F)** Representative images and quantification from immunofluorescence on spheroids for fibronectin (**E**), integrin B4 (**E**), and integrin AV (**F**). One independent experiment of each. **G)** Quantification of spheroid size after immunofluorescence processing. One of 4 independent experiments is shown. One-way ANOVA. ns = not significant, *p < 0.05, ***p < 0.001, ****p < 0.0001.

immunofluorescence. We observed decreased levels fibronectin and both integrins B4 and AV (**Fig. 4D-F**). Heat inactivated SCM did not differ from whole SCM, indicating this decrease is not due to MMP-induced remodeling and that SASP induces cell intrinsic decrease in adhesion and spheroid structure. Interestingly, although the spheroids compact to the same size, regardless of conditioned media composition (**Fig. 2E-F**), spheroids cultured in SCM expanded during the immunofluorescence processing and were on average larger than control PCM-cultured spheroids (**Fig. 4G**). This is consistent with the observation that spheroids cultured in SCM are more loosely attached than those cultured in PCM. These data support the conclusion that the SASP decreases adhesion factor expression in spheroids, which is likely independent of MMP degradation.

DISCUSSION

HGSOC is aggressive in nature with a high metastatic potential. The phenomenon of senescence has gained increasing attention in cancer research due to its complex role influencing the tumor microenvironment through the SASP. In this study, we investigated the impact of senescent cells and their SASP on HGSOC to better understand the effects of chemotherapy on adhesion and detachment using spheroids as an *in vitro* model system. Our results indicate that the SASP decreases spheroid attachment and increases detachment events, which correlates with cellular detachment and downregulation of ECM and adhesion factors. These studies may have significant implications for HGSOC progression.

Components of the SASP have been linked to metastasis in various cell and cancer types (Coppe et al. 2010). In pancreatic cancer, hepatocyte growth factor drives cancer dissemination (Ohuchida et al. 2004). Similarly, IL-6 and IL-8 in the SASP of senescent fibroblasts enhance breast cancer cell invasion (Rodier and Goldstein 2008). In ovarian cancer, a number SASP effectors have been linked to ovarian cancer dissemination, although these studies are not specifically related to senescence (Veenstra, Bittencourt, and Aird 2022). IL-6 further enriches ovarian cancer stem cells, which are known to promote dissemination (Zong and Nephew 2019). IL-8 expression is associated with ovarian cancer dissemination (Wen et al. 2020) and is higher in the ascites of late stage (stage III/IV) ovarian cancer patients (Zhang et al. 2019). The malignant ascites from late stage ovarian cancer patients, containing various cytokines often expressed in the SASP (Matte et al. 2012), can promote adhesion and migration through the mesothelium (Mikuła-Pietrasik et al. 2016). Our data support the conclusion that cisplatin-induced senescence induction in ovarian cancer directly affects adhesion and detachment in spheroids, which may help promote metastasis. Studies using SCM *in vivo* are required to fully assess the contribution of the SASP in dissemination of HGSOC.

Our data suggest that the enhanced cellular detachment from spheroids can be induced by the SASP in an MMP-independent mechanism. MMPs are well-known contributors to cancer cell invasion and metastasis (Gonzalez-Avila et al. 2019), and MMP1, 3, 10, 12, 13, and 14 are associated with SASP (Coppe et al. 2010). In ovarian cancer, MMP3 is associated with late stage disease (Wang et al. 2019), and both MMP1 and MMP3 promote ovarian cancer dissemination (Agarwal et al. 2008). We did not observe marked differences in the expression of MMPs (**Table S2**). Moreover, heat inactivation of SCM to denature MMPs did not rescue the changes in spheroid adhesion (**Fig. 2B-D**) or cellular detachment (**Fig. 3B-C**), indicating cell-intrinsic changes in the ECM and adhesion factor expression also contribute to HGSOC dissemination. This is consistent with findings in other models that the SASP can lead to remodeling of the ECM and alterations in cell-cell and cell-ECM interactions (Ghosh et al. 2020; Mavrogonatou et al. 2023). Such changes can affect cellular adhesion and motility, key events in the metastatic cascade. Further experiments are warranted to uncover the precise components of the SASP driving these molecular changes and the underlying mechanism of subsequent cell detachment.

It is interesting to speculate whether these changes in adhesion and detachment observed in cells cultured in SCM could be therapeutically targeted. One such therapeutic route is the use of senolytics, a class of drugs designed to selectively target and eliminate senescent cells (Kirkland and Tchkonia 2020). In the context of cancer, selective killing of senescent cells has exhibited anti-tumor effects, including suppressing metastasis (Demaria et al. 2017). While the application of senolytics in ovarian cancer remains largely unexplored, the potential benefits are underscored by their success in other cancer types. In breast cancer, GL-V9 has been shown to preferentially kill both senescent breast cancer cells and replication-induced senescent fibroblasts (Yang et al. 2021), and its use has been shown to decrease invasion and metastasis (Li

et al. 2011). Similarly, the senolytic Digitonin has been shown to be an effective complement to chemotherapy in breast cancer treatment (Triana-Martínez et al. 2019). Several senolytic agents are undergoing clinical trials, demonstrating the growing interest in their therapeutic potential (Zhang et al. 2023). The translation of these findings to ovarian cancer could represent a novel therapeutic strategy to specifically target senescent cells and mitigate the metastatic potential induced by the SASP.

In summary, this study sheds light on a previously unexplored facet of ovarian cancer by revealing how the SASP of senescent cells contributes to HGSOC phenotypes. The SASP-induced changes in cellular detachment from spheroids, along with cell-intrinsic alterations in ECM and adhesion factor expression, provide a novel perspective on the complex interplay between senescence and cancer progression. These findings underscore the importance of understanding the SASP and its multifaceted impact on the tumor microenvironment, offering potential therapeutic targets for mitigating ovarian cancer metastasis.

Materials and Methods

Cell Lines

Ovcar8 cells were a gift from Dr. Benjamin Bitler (University of Colorado). Kuramochi cells were a gift from Dr. Rugang Zhang (The Wistar Institute). All cells were cultured in RPMI 1640 (Fisher Scientific cat#) supplemented with 5% Fetal Bovine Serum (BioWest, cat# S1620) and 1% Penicillin/Streptomycin (Fisher Scientific, cat#15-140-122) unless otherwise noted. All cell lines were tested monthly for mycoplasma as described in (Uphoff and Drexler 2005).

Senescence induction and conditioned media generation

Cells were treated with 1 μM cisplatin (Selleck Chemicals, cat#S1166) or vehicle for 48 hours, after which the cisplatin treated cells were washed with PBS and cultured in fresh media. Vehicle treated cells were split into fresh media. After 24 hours, the media was changed and allowed to condition for 48 hours. Conditioned media was collected and filtered with a 0.22 μm sterile vacuum filter (Fisher Scientific, cat#FB12566506) and stored at -80° C.

Proliferation assays

An equal number of cells were seeded in multiwell plates and cultured for 4-5 days. Proliferation was assessed by fixing the plates for 5 min with 1% paraformaldehyde after which they were stained with 0.05% crystal violet. Wells were destained using 10% acetic acid. Absorbance (590nm) was measured using a spectrophotometer (BioTek Epoch Microplate reader).

Senescence Associated-β-Galactosidase assay

SA-β-Gal staining was performed as previously described (Dimri et al. 1995). Cells were fixed in 2% formaldehyde/0.2% glutaraldehyde in PBS (5 min) and stained (40 mM Na_2HPO_4, 150 mM NaCl, 2 mM $MgCl_2$, 5 mM $K_3Fe(CN)_6$, 5 mM $K_4Fe(CN)_6$, and 1 mg/ml X-gal) overnight at 37°C

in a non-CO2 incubator. Images were acquired at room temperature using an inverted microscope (Nikon Eclipse Ts2) with a 20X/0.40 objective (Nikon LWD) equipped with a camera (Nikon DS-Fi3). Each sample was assessed in triplicate and at least 100 cells per well were counted (> 300 cells per experiment).

RNA isolation, Sequencing, and Analysis

Total RNA was extracted from cells with Trizol (Ambion, cat#15596018) and DNase treated, cleaned, and concentrated using Zymo columns (Zymo Research, cat#R1013) following manufacturer's instructions. RNA integrity number (RIN) was measured using BioAnalyzer (Agilent Technologies) RNA 6000 Nano Kit to confirm RIN above 7 for each sample. The cDNA libraries, next generation sequencing, and bioinformatics analysis was performed by Novogene. Raw and processed RNA-Seq data can be found on GEO (GSE248979 and GSE248930).

RT-qPCR

RNA was retrotranscribed with High-Capacity cDNA Reverse Transcription Kit (Applied Biosystems, cat#4368814) and 20ng of cDNA amplified using the CFX Connect Real-time PCR system (Bio-Rad) and the PowerUp™ SYBR™ Green Master Mix (Applied Biosystems, cat#A25742) following manufacturer's instructions. Primers were designed using the Integrated DNA Technologies (IDT) web tool (*IL1A*: 5' GGTTGAGTTTAAGCCAATCCA, 3' TGCTGACCTAGGCTTGATGA; *IL1B*: 5' CTGTCCTGCGTGTTGAAAGA, 3' TTGGGTAATTTTTGGGATCTACA; *IL6*: 5' AAAAGTCCTGATCCAGTTCCTG, 3' TGAGTTGTCATGTCCTGCAG; *CXCL8*: 5' GAGAGTGATTGAGAGTGGACCAC, 3' CACAACCCTCTGCACCCAGTTT). Conditions for amplification were: 5 min at 95° C, 40 cycles of 10 sec at 95° C and 7 sec at 62° C. The assay ended with a melting curve program: 15 sec at 95° C, 1 min at 70° C, then ramping to 95° C while continuously monitoring fluorescence. Each sample was assessed in triplicate. Relative quantification was

determined to multiple reference genes (*PSMC4* [5' TGTTGGCAAAGGCGGTGGCA, 3' TCTCTTGGTGGCGATGGCAT], and *MRPL9* [5' CAGTTTCTGGGGATTTGCAT, 3' TATTCAG-GAAGGGCATCTCG]) to ensure reproducibility using the delta-delta CT method.

Cytokine array

The human cytokine antibody array C1000 (RayBio, cat# AAH-CYT-1000-2) was used to quantify secreted factors as we have previously published (Leon et al. 2021). Conditioned medias were obtained as described above. Membranes were visualized on film. Individual spot signal densities were obtained using ImageJ software and normalized to cell number from which the conditioned media were obtained.

Immunofluorescence imaging

For immunofluorescence of adherent cells, cells were seeded at an equal density on coverslips and fixed with 4% paraformaldehyde. Cells were washed four times with 1× PBS and permeabilized with 0.2% Triton X-100 in PBS for 5 min and then postfixed with 1% paraformaldehyde and 0.01% Tween 20 for 30 min. Cells were blocked for 5 min with 3% BSA/PBS followed by incubation of corresponding primary antibody in 3% BSA/PBS for 1 h at room temperature. Prior to incubation with secondary antibody in 3% BSA/PBS for 1 h at room temperature, cells were washed three times with 1% Triton X-100 in PBS. Cells were then incubated with 0.15 µg/ml DAPI in 1× PBS for 1 min, washed three times with 1× PBS, mounted with fluorescence mounting medium (9 ml of glycerol [BP229-1; Fisher Scientific], 1 ml of 1× PBS, and 10 mg of p-phenylenediamine [PX0730; EMD Chemicals]; pH was adjusted to 8.0–9.0 using carbonate-bicarbonate buffer [0.2 M anhydrous sodium carbonate, 0.2 M sodium bicarbonate]) and sealed. At least 200 cells per coverslip were counted. Images were obtained at room temperature using a Nikon ECLIPSE Ti2 microscope with a 20×/0.17 objective (Nikon DIC N2 Plan Apo) equipped

with a camera (ORCA-Fusion C14440). Images were acquired using NIS-Elements AR software and processed using ImageJ.

For immunofluorescence on nonadherent cells, spheroids formed in round bottom ULA were fixed in 4% paraformaldehyde and permeabilized with 0.5% Triton-X 100 in TBS for 30 minutes rotating at room temperature. Spheroids were blocked for 1 hour in 5% normal donkey serum, 2% BSA, 0.1% Triton X-100 in TBS rotating at room temperature. Primary antibody was added and incubated rotating at 4° C for 18 hours. Prior to incubation with secondary antibody in 1 hour in 5% normal donkey serum, 2% BSA, 0.1% Triton X-100 in TBS for 3 hours at room temperature, cells were washed three times with 0.1% Triton X-100 in TBS. Spheroids were then incubated with 300nM DAPI in 0.1% Triton X-100 in TBS for 15 minutes, washed three times with 0.1% Triton X-100 in TBS, mounted with fluorescence mounting medium (9 ml of glycerol [Fisher Scientific cat#BP229-1], 1 ml of 1× PBS, and 10 mg of p-phenylenediamine [EMD Chemicals, cat# PX0730]; pH was adjusted to 8.0–9.0 using carbonate-bicarbonate buffer [0.2 M anhydrous sodium carbonate, 0.2 M sodium bicarbonate]) and sealed. Z-stacked images were taken with a Leica Thunder Imager and Nikon AXR point scanning confocal microscope with a 20x objective and processed using ImageJ. Fluorescence intensity was determined using a manual fixed threshold for all images with the exception of Integrin AV, where automated thresholding was used.

Non-adherent culture and imaging

Non-adherent cell culture and imaging was performed as previously described (Shonibare et al. 2022). Briefly, cells were seeded 1,000 (96 well round bottom ULA, Corning cat#), 10,000 (96 well flat bottom ULA, Corning cat#), or 300,000 (6 well flat bottom ULA, Corning cat#) cells per well in a 1:1 ratio of fresh to conditioned media. To assess viability, cells were treated with 1 μM

ethidium homodimer (Sigma Aldrich, cat# 46043) and 0.5 μM calcein AM (Invitrogen, cat#C1430) for 30 minutes and images were acquired using a Leica Thunder Imager. Timelapse imaging to assess spheroid formation in round bottom ULA plates was performed using IncuCyte S3 imaging system (Sartorius). Cells were seeded in 96 well ULA plates and images every 3 hours for 48 hours. Timelapse imaging of spheroids to assess detachment was performed using a Leica Thunder Imager with a Okolab incubation chamber. Spheroids formed in round bottom ULA culture in the presence of conditioned media were transferred to a flat bottom ULA plate, treated with 0.5 μM calcein AM, and Z-stacked images were acquired every 15 minutes for 12 hours.

Quantification and Statistical Analysis

GraphPad Prism (version 10.0) was used to perform statistical analysis. Point estimates with standard deviations or standard errors were reported, as indicated, and the appropriate statistical test was performed using all observed experimental data. All statistical tests performed were two-sided and p-values < 0.05 were considered statistically significant. When necessary, outliers were identified and excluded by the ROUT method ($Q = 0.1\%$).

SUPPLEMENTAL FIGURE

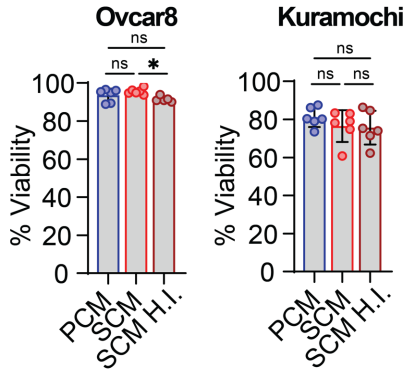

Figure S1. Anoikis resistance is not conferred by the SASP in HGSOC cells. Percentage of live cell area over total area determined by fluorescent staining with calcein AM live cell fluorescence stain and ethidium homodimer dead cell fluorescent stain (representative images in **Fig. 2B**). One of 5 independent experiments in Ovcar8 and 3 independent experiments in Kuramochi is shown. One-way ANOVA. ns = not significant. *p<0.05

Acknowledgements

We thank Dr. Yannis Zervantonakis and Dr. Adam Straub (University of Pittsburgh) for reagents. This work was supported by grants from the National Institutes of Health (R37CA240625 to K.M.A., R01CA259111 to K.M.A., and T32GM133332 to A.R.C.), the Melanoma Research Foundation (to R.B.G.), and the Ovarian Cancer Research Alliance (MIG-2023-2-1018 to A.U.).

Author Contributions

Aidan R. Cole: Conceptualization, Investigation, Methodology, Writing – Original Draft, Visualization, Writing – Review & Editing. **Raquel Buj:** Investigation, Methodology, Writing – Review & Editing. **Amal Taher Elhaw:** Methodology, Writing – Review & Editing. **Apoorva Uboveja:** Investigation, Writing – Review & Editing. **Naveen Kumar Tangudu:** Investigation, Writing – Review & Editing. **Steffi Oesterreich:** Writing – Review & Editing. **Wayne Stallaert:** Investigation, Methodology, Writing – Review & Editing. **Nadine Hempel:** Methodology, Supervision, Writing – Review & Editing. **Katherine M. Aird:** Conceptualization, Visualization, Writing – Original Draft, Writing – Review & Editing, Supervision, Project Administration, Funding Acquisition.

Declaration of Interests

All authors declare no competing interests.

References

Acosta, J. C., and J. Gil. 2012. 'Senescence: a new weapon for cancer therapy', *Trends Cell Biol*, 22: 211-9.

Agarwal, Anika, Lidija Covic, Leila M Sevigny, Nicole C Kaneider, Katherine Lazarides, Gissou Azabdaftari, Sheida Sharifi, and Athan Kuliopulos. 2008. 'Targeting a metalloprotease-PAR1 signaling system with cell-penetrating pepducins inhibits angiogenesis, ascites, and progression of ovarian cancer', *Molecular cancer therapeutics*, 7: 2746-57.

Al Habyan, Sara, Christina Kalos, Joseph Szymborski, and Luke McCaffrey. 2018. 'Multicellular detachment generates metastatic spheroids during intra-abdominal dissemination in epithelial ovarian cancer', *Oncogene*, 37: 5127-35.

Alimirah, F., T. Pulido, A. Valdovinos, S. Alptekin, E. Chang, E. Jones, D. A. Diaz, J. Flores, M. C. Velarde, M. Demaria, A. R. Davalos, C. D. Wiley, C. Limbad, P. Y. Desprez, and J. Campisi. 2020. 'Cellular Senescence Promotes Skin Carcinogenesis through p38MAPK and p44/42MAPK Signaling', *Cancer Res*, 80: 3606-19.

Amate, P., C. Huchon, A. L. Dessapt, C. Bensaid, J. Medioni, M. A. Le Frere Belda, A. S. Bats, and F. R. Lecuru. 2013. 'Ovarian cancer: sites of recurrence', *Int J Gynecol Cancer*, 23: 1590-6.

Boylan, Kristin LM, Rory D Manion, Heena Shah, Keith M Skubitz, and Amy PN Skubitz. 2020. 'Inhibition of ovarian cancer cell spheroid formation by synthetic peptides derived from Nectin-4', *International Journal of Molecular Sciences*, 21: 4637.

Camphausen, Kevin, Marsha A Moses, Wolf-Dietrich Beecken, Mohamed K Khan, Judah Folkman, and Michael S O'Reilly. 2001. 'Radiation therapy to a primary tumor accelerates metastatic growth in mice', *Cancer research*, 61: 2207-11.

Casagrande, Naike, Cinzia Borghese, Francesco Agostini, Cristina Durante, Mario Mazzucato, Alfonso Colombatti, and Donatella Aldinucci. 2021. 'In ovarian cancer multicellular spheroids, platelet releasate promotes growth, expansion of ALDH+ and CD133+ cancer stem cells, and protection against the cytotoxic effects of cisplatin, carboplatin and paclitaxel', *International Journal of Molecular Sciences*, 22: 3019.

Coccolini, F., F. Gheza, M. Lotti, S. Virzì, D. Iusco, C. Ghermandi, R. Melotti, G. Baiocchi, S. M. Giulini, L. Ansaloni, and F. Catena. 2013. 'Peritoneal carcinomatosis', *World J Gastroenterol*, 19: 6979-94.

Comamala, M., M. Pinard, C. Thériault, I. Matte, A. Albert, M. Boivin, J. Beaudin, A. Piché, and C. Rancourt. 2011. 'Downregulation of cell surface CA125/MUC16 induces epithelial-to-mesenchymal transition and restores EGFR signalling in NIH:OVCAR3 ovarian carcinoma cells', *Br J Cancer*, 104: 989-99.

Coppe, J. P., P. Y. Desprez, A. Krtolica, and J. Campisi. 2010. 'The senescence-associated secretory phenotype: the dark side of tumor suppression', *Annu Rev Pathol*, 5: 99-118.

Davidson, Ben, Virginia Espina, Seth M. Steinberg, Vivi Ann Flørenes, Lance A. Liotta, Gunnar B. Kristensen, Claes G. Tropé, Aasmund Berner, and Elise C. Kohn. 2006. 'Proteomic Analysis of Malignant Ovarian Cancer Effusions as a Tool for Biologic and Prognostic Profiling', *Clinical Cancer Research*, 12: 791-99.

Della Pepa, Chiara, Giuseppe Tonini, Carmela Pisano, Marilena Di Napoli, Sabrina Chiara Cecere, Rosa Tambaro, Gaetano Facchini, and Sando Pignata. 2015. 'Ovarian cancer standard of care: are there real alternatives?', *Chinese journal of cancer*, 34: 17-27.

Demaria, M., M. N. O'Leary, J. Chang, L. Shao, S. Liu, F. Alimirah, K. Koenig, C. Le, N. Mitin, A. M. Deal, S. Alston, E. C. Academia, S. Kilmarx, A. Valdovinos, B. Wang, A. de Bruin, B. K. Kennedy, S. Melov, D. Zhou, N. E. Sharpless, H. Muss, and J. Campisi. 2017. 'Cellular

Senescence Promotes Adverse Effects of Chemotherapy and Cancer Relapse', *Cancer Discov*, 7: 165-76.

Dimri, G. P., X. Lee, G. Basile, M. Acosta, G. Scott, C. Roskelley, E. E. Medrano, M. Linskens, I. Rubelj, O. Pereira-Smith, and et al. 1995. 'A biomarker that identifies senescent human cells in culture and in aging skin in vivo', *Proc Natl Acad Sci U S A*, 92: 9363-7.

Fleury, H., N. Malaquin, V. Tu, S. Gilbert, A. Martinez, M. A. Olivier, A. Sauriol, L. Communal, K. Leclerc-Desaulniers, E. Carmona, D. Provencher, A. M. Mes-Masson, and F. Rodier. 2019. 'Exploiting interconnected synthetic lethal interactions between PARP inhibition and cancer cell reversible senescence', *Nat Commun*, 10: 2556.

Fujimoto, J., S. Ichigo, R. Hirose, H. Sakaguchi, and T. Tamaya. 1997. 'Expression of E-cadherin and alpha- and beta-catenin mRNAs in ovarian cancers', *Cancer Lett*, 115: 207-12.

Ghosh, D., C. Mejia Pena, N. Quach, B. Xuan, A. H. Lee, and M. R. Dawson. 2020. 'Senescent mesenchymal stem cells remodel extracellular matrix driving breast cancer cells to a more-invasive phenotype', *J Cell Sci*, 133.

Gonzalez-Avila, Georgina, Bettina Sommer, Daniel A. Mendoza-Posada, Carlos Ramos, A. Armando Garcia-Hernandez, and Ramces Falfan-Valencia. 2019. 'Matrix metalloproteinases participation in the metastatic process and their diagnostic and therapeutic applications in cancer', *Critical Reviews in Oncology/Hematology*, 137: 57-83.

Kalathur, Madhuri, Diletta Di Mitri, and Andrea Alimonti. 2015. 'Pro-senescence Therapy for Cancer: Time for the Clinic.' in Georg T. Wondrak (ed.), *Stress Response Pathways in Cancer: From Molecular Targets to Novel Therapeutics* (Springer Netherlands: Dordrecht).

Kipps, Emma, David S. P. Tan, and Stan B. Kaye. 2013. 'Meeting the challenge of ascites in ovarian cancer: new avenues for therapy and research', *Nature Reviews Cancer*, 13: 273-82.

Kirkland, J. L., and T. Tchkonia. 2020. 'Senolytic drugs: from discovery to translation', *J Intern Med*, 288: 518-36.

Krtolica, Ana, Simona Parrinello, Stephen Lockett, Pierre-Yves Desprez, and Judith Campisi. 2001. 'Senescent fibroblasts promote epithelial cell growth and tumorigenesis: a link between cancer and aging', *Proceedings of the National Academy of Sciences*, 98: 12072-77.

Kuilman, T., C. Michaloglou, L. C. Vredeveld, S. Douma, R. van Doorn, C. J. Desmet, L. A. Aarden, W. J. Mooi, and D. S. Peeper. 2008. 'Oncogene-induced senescence relayed by an interleukin-dependent inflammatory network', *Cell*, 133: 1019-31.

Lane, Denis, Isabelle Matte, Claudine Rancourt, and Alain Piché. 2011. 'Prognostic significance of IL-6 and IL-8 ascites levels in ovarian cancer patients', *BMC cancer*, 11: 1-6.

Latifi, A., R. B. Luwor, M. Bilandzic, S. Nazaretian, K. Stenvers, J. Pyman, H. Zhu, E. W. Thompson, M. A. Quinn, J. K. Findlay, and N. Ahmed. 2012. 'Isolation and characterization of tumor cells from the ascites of ovarian cancer patients: molecular phenotype of chemoresistant ovarian tumors', *PLoS One*, 7: e46858.

Lau, M. T., W. K. So, and P. C. Leung. 2013. 'Fibroblast growth factor 2 induces E-cadherin down-regulation via PI3K/Akt/mTOR and MAPK/ERK signaling in ovarian cancer cells', *PLOS ONE*, 8: e59083.

Lee, M. Y., C. Y. Chou, M. J. Tang, and M. R. Shen. 2008. 'Epithelial-mesenchymal transition in cervical cancer: correlation with tumor progression, epidermal growth factor receptor overexpression, and snail up-regulation', *Clin Cancer Res*, 14: 4743-50.

Lengyel, E. 2010. 'Ovarian cancer development and metastasis', *Am J Pathol*, 177: 1053-64.

Leon, K. E., R. Buj, E. Lesko, E. S. Dahl, C. W. Chen, N. K. Tangudu, Y. Imamura-Kawasawa, A. V. Kossenkov, R. P. Hobbs, and K. M. Aird. 2021. 'DOT1L modulates the senescence-associated secretory phenotype through epigenetic regulation of IL1A', *J Cell Biol*, 220.

Li, L., P. Chen, Y. Ling, X. Song, Z. Lu, Q. He, Z. Li, N. Lu, and Q. Guo. 2011. 'Inhibitory effects of GL-V9 on the invasion of human breast carcinoma cells by downregulating the expression and activity of matrix metalloproteinase-2/9', *Eur J Pharm Sci*, 43: 393-9.

Liu, Dan, and Peter J Hornsby. 2007. 'Senescent human fibroblasts increase the early growth of xenograft tumors via matrix metalloproteinase secretion', *Cancer research*, 67: 3117-26.

Matte, I., D. Lane, C. Laplante, C. Rancourt, and A. Piché. 2012. 'Profiling of cytokines in human epithelial ovarian cancer ascites', *Am J Cancer Res*, 2: 566-80.

Mavrogonatou, E., A. Papadopoulou, H. Pratsinis, and D. Kletsas. 2023. 'Senescence-associated alterations in the extracellular matrix: deciphering their role in the regulation of cellular function', *Am J Physiol Cell Physiol*, 325: C633-c47.

McPherson, A., A. Roth, E. Laks, T. Masud, A. Bashashati, A. W. Zhang, G. Ha, J. Biele, D. Yap, A. Wan, L. M. Prentice, J. Khattra, M. A. Smith, C. B. Nielsen, S. C. Mullaly, S. Kalloger, A. Karnezis, K. Shumansky, C. Siu, J. Rosner, H. L. Chan, J. Ho, N. Melnyk, J. Senz, W. Yang, R. Moore, A. J. Mungall, M. A. Marra, A. Bouchard-Côté, C. B. Gilks, D. G. Huntsman, J. N. McAlpine, S. Aparicio, and S. P. Shah. 2016. 'Divergent modes of clonal spread and intraperitoneal mixing in high-grade serous ovarian cancer', *Nat Genet*, 48: 758-67.

Mehner, C., E. Miller, A. Hockla, M. Coban, S. J. Weroha, D. C. Radisky, and E. S. Radisky. 2020. 'Targeting an autocrine IL-6-SPINK1 signaling axis to suppress metastatic spread in ovarian clear cell carcinoma', *Oncogene*, 39: 6606-18.

Meraz-Cruz, N., F. Vadillo-Ortega, A. M. Jiménez-Garduño, and A. Ortega. 2020. 'Thermal stability of human matrix metalloproteinases', *Heliyon*, 6: e03865.

Mikuła-Pietrasik, Justyna, Paweł Uruski, Kinga Matuszkiewicz, Sebastian Szubert, Rafał Moszyński, Dariusz Szpurek, Stefan Sajdak, Andrzej Tykarski, and Krzysztof Książek. 2016. 'Ovarian cancer-derived ascitic fluids induce a senescence-dependent pro-cancerogenic phenotype in normal peritoneal mesothelial cells', *Cellular Oncology*, 39: 473-81.

Myong, N. H. 2012. 'Loss of E-cadherin and Acquisition of Vimentin in Epithelial-Mesenchymal Transition are Noble Indicators of Uterine Cervix Cancer Progression', *Korean J Pathol*, 46: 341-8.

Ohuchida, Kenoki, Kazuhiro Mizumoto, Mitsuhiko Murakami, Li-Wu Qian, Norihiro Sato, Eishi Nagai, Kunio Matsumoto, Toshikazu Nakamura, and Masao Tanaka. 2004. 'Radiation to stromal fibroblasts increases invasiveness of pancreatic cancer cells through tumor-stromal interactions', *Cancer research*, 64: 3215-22.

Paffenholz, S. V., C. Salvagno, Y. J. Ho, M. Limjoco, T. Baslan, S. Tian, A. Kulick, E. de Stanchina, J. E. Wilkinson, F. M. Barriga, D. Zamarin, J. R. Cubillos-Ruiz, J. Leibold, and S. W. Lowe. 2022. 'Senescence induction dictates response to chemo- and immunotherapy in preclinical models of ovarian cancer', *Proc Natl Acad Sci U S A*, 119.

Parrinello, Simona, Jean-Philippe Coppe, Ana Krtolica, and Judith Campisi. 2005. 'Stromal-epithelial interactions in aging and cancer: senescent fibroblasts alter epithelial cell differentiation', *Journal of cell science*, 118: 485-96.

Perez-Mancera, P. A., A. R. Young, and M. Narita. 2014. 'Inside and out: the activities of senescence in cancer', *Nat Rev Cancer*, 14: 547-58.

Qian, Li-Wu, Kazuhiro Mizumoto, Taro Urashima, Eishi Nagai, Naoki Maehara, Norihiro Sato, Motowo Nakajima, and Masao Tanaka. 2002. 'Radiation-induced increase in invasive

potential of human pancreatic cancer cells and its blockade by a matrix metalloproteinase inhibitor, CGS27023', *Clinical Cancer Research*, 8: 1223-27.

Ritch, Sabrina J., Abu Shadat M. Noman, Alicia A. Goyeneche, and Carlos M. Telleria. 2022. 'The metastatic capacity of high-grade serous ovarian cancer cells changes along disease progression: inhibition by mifepristone', *Cancer Cell International*, 22: 397.

Ritschka, B., M. Storer, A. Mas, F. Heinzmann, M. C. Ortells, J. P. Morton, O. J. Sansom, L. Zender, and W. M. Keyes. 2017. 'The senescence-associated secretory phenotype induces cellular plasticity and tissue regeneration', *Genes Dev*, 31: 172-83.

Rodier, JP Coppé CK Patil F, and Y Sun DP Muñoz J Goldstein. 2008. 'Senescence-associated secretory phenotypes reveal cell-nonautonomous functions of oncogenic RAS and the p53 tumor suppressor', *PLoS Biol*, 6: 2853-68.

Sawada, K., A. K. Mitra, A. R. Radjabi, V. Bhaskar, E. O. Kistner, M. Tretiakova, S. Jagadeeswaran, A. Montag, A. Becker, H. A. Kenny, M. E. Peter, V. Ramakrishnan, S. D. Yamada, and E. Lengyel. 2008. 'Loss of E-cadherin promotes ovarian cancer metastasis via alpha 5-integrin, which is a therapeutic target', *Cancer Res*, 68: 2329-39.

Shonibare, Zainab, Mehri Monavarian, Kathleen O'Connell, Diego Altomare, Abigail Shelton, Shubham Mehta, Renata Jaskula-Sztul, Rebecca Phaeton, Mark D. Starr, Regina Whitaker, Andrew Berchuck, Andrew B. Nixon, Rebecca C. Arend, Nam Y. Lee, C. Ryan Miller, Nadine Hempel, and Karthikeyan Mythreye. 2022. 'Reciprocal SOX2 regulation by SMAD1-SMAD3 is critical for anoikis resistance and metastasis in cancer', *Cell Reports*, 40: 111066.

Singh, Manu Smriti, Meir Goldsmith, Kavita Thakur, Sushmita Chatterjee, Dalit Landesman-Milo, Tally Levy, Leoni A Kunz-Schughart, Yechezkel Barenholz, and Dan Peer. 2020. 'An ovarian spheroid based tumor model that represents vascularized tumors and enables the investigation of nanomedicine therapeutics', *Nanoscale*, 12: 1894-903.

Sparmann, A., and D. Bar-Sagi. 2004. 'Ras-induced interleukin-8 expression plays a critical role in tumor growth and angiogenesis', *Cancer Cell*, 6: 447-58.

Tan, D. S., R. Agarwal, and S. B. Kaye. 2006. 'Mechanisms of transcoelomic metastasis in ovarian cancer', *Lancet Oncol*, 7: 925-34.

Torre, L. A., B. Trabert, C. E. DeSantis, K. D. Miller, G. Samimi, C. D. Runowicz, M. M. Gaudet, A. Jemal, and R. L. Siegel. 2018. 'Ovarian cancer statistics, 2018', *CA Cancer J Clin*, 68: 284-96.

Triana-Martínez, F., P. Picallos-Rabina, S. Da Silva-Álvarez, F. Pietrocola, S. Llanos, V. Rodilla, E. Soprano, P. Pedrosa, A. Ferreirós, M. Barradas, F. Hernández-González, M. Lalinde, N. Prats, C. Bernadó, P. González, M. Gómez, M. P. Ikonomopoulou, P. J. Fernández-Marcos, T. García-Caballero, P. Del Pino, J. Arribas, A. Vidal, M. González-Barcia, M. Serrano, M. I. Loza, E. Domínguez, and M. Collado. 2019. 'Identification and characterization of Cardiac Glycosides as senolytic compounds', *Nat Commun*, 10: 4731.

Tsai, Kelvin KC, Eric Yao-Yu Chuang, John B Little, and Zhi-Min Yuan. 2005. 'Cellular mechanisms for low-dose ionizing radiation–induced perturbation of the breast tissue microenvironment', *Cancer research*, 65: 6734-44.

Uphoff, C. C., and H. G. Drexler. 2005. 'Detection of mycoplasma contaminations', *Methods Mol Biol*, 290: 13-23.

Valmiki, S., M. A. Aid, A. R. Chaitou, M. Zahid, M. Valmiki, P. Fawzy, and S. Khan. 2021. 'Extracellular Matrix: A Treasure Trove in Ovarian Cancer Dissemination and Chemotherapeutic Resistance', *Cureus*, 13: e13864.

Veenstra, J. P., L. F. F. Bittencourt, and K. M. Aird. 2022. 'The Senescence-Associated Secretory Phenotype in Ovarian Cancer Dissemination', *Am J Physiol Cell Physiol*.

Wang, Shujie, Jia Jia, Dongyan Liu, Meng Wang, Zhen Wang, Xueling Li, Hongzhi Wang, Yong Rui, Zhirong Liu, and Wei Guo. 2019. 'Matrix metalloproteinase expressions play important role in prediction of ovarian cancer outcome', *Scientific reports*, 9: 11677.

Wen, Jirui, Zhiwei Zhao, Liwei Huang, Ling Wang, Yali Miao, and Jiang Wu. 2020. 'IL-8 promotes cell migration through regulating EMT by activating the Wnt/β-catenin pathway in ovarian cancer', *Journal of Cellular and Molecular Medicine*, 24: 1588-98.

Wen, Wei, Wei Liang, Jun Wu, Claudia M Kowolik, Ralf Buettner, Anna Scuto, Meng-Yin Hsieh, Hao Hong, Christine E Brown, and Stephen J Forman. 2014. 'Targeting JAK1/STAT3 signaling suppresses tumor progression and metastasis in a peritoneal model of human ovarian cancer', *Molecular cancer therapeutics*, 13: 3037-48.

Wiley, C. D., M. C. Velarde, P. Lecot, S. Liu, E. A. Sarnoski, A. Freund, K. Shirakawa, H. W. Lim, S. S. Davis, A. Ramanathan, A. A. Gerencser, E. Verdin, and J. Campisi. 2016. 'Mitochondrial Dysfunction Induces Senescence with a Distinct Secretory Phenotype', *Cell Metab*, 23: 303-14.

Yang, D., X. Tian, Y. Ye, Y. Liang, J. Zhao, T. Wu, and N. Lu. 2021. 'Identification of GL-V9 as a novel senolytic agent against senescent breast cancer cells', *Life Sci*, 272: 119196.

Yee, Christine, Kristie-Ann Dickson, Mohammed N. Muntasir, Yue Ma, and Deborah J. Marsh. 2022. 'Three-Dimensional Modelling of Ovarian Cancer: From Cell Lines to Organoids for Discovery and Personalized Medicine', *Frontiers in Bioengineering and Biotechnology*, 10.

Zhang, Lei, Louise E. Pitcher, Vaishali Prahalad, Laura J. Niedernhofer, and Paul D. Robbins. 2023. 'Targeting cellular senescence with senotherapeutics: senolytics and senomorphics', *The FEBS Journal*, 290: 1362-83.

Zhang, Lixia, Weiwei Liu, Xinbo Wang, Xiaoli Wang, and Hong Sun. 2019. 'Prognostic value of serum IL-8 and IL-10 in patients with ovarian cancer undergoing chemotherapy', *Oncology Letters*, 17: 2365-69.

Zong, Xingyue, and Kenneth P Nephew. 2019. 'Ovarian cancer stem cells: role in metastasis and opportunity for therapeutic targeting', *Cancers*, 11: 934.